ON THE WEAKNESSES OF TRADITIONAL WAVE NUMBER ANALYSIS AND ITS IMPACT IN THE DEVELOPMENT OF ACCURATE CONVECTION DISCRETIZATION

Luiz Eduardo Bittencourt Sampaio, luizebs@vm.uff.br
Universidade Federal Fluminense (UFF) – LMTA/PGMEC
Rua Passo da Pátria 156, bloco E, sala 216, Niterói, RJ, 24210-240, Brazil

Abstract. Several numerical schemes have been proposed in the literature to deal with convection phenomena, but all of them present some spurious dispersion and/or diffusion. These spurious effects can in principle be made as small as desired, but at the price of increasing the computational stencil and the computational cost. Usually, wave number technique is the method of choice to analyze numerical errors and to help design better schemes. This analysis is however restricted to a certain interval in time, and the calculated error is therefore cummulative. This paper main objectives are two fold: 1) to discuss the main weaknesses of traditional wave number analysis and how this have hampered the development of more accurate schemes; 2) to propose a better strategy for error assessment that will ultimately lead to the development of a new family of numerical schemes that can provide a significant increase in accuracy when dealing with the convection phenomena. The general framework for the development of better schemes is presented and the impact on key areas of computational physics, like aero-acoustics, turbulence modeling and multiphase flows, is discussed.

Keywords: Numerical schemes, convection, dispersion, diffusion, CFD

1. INTRODUCTION

Convective transport is present in many physical phenomena involving fluids. Its numerical simulation has been one of the key challenges in Computational Physics and the subject of many investigations since the earlier days of Computational Fluid Dynamics (CFD) (van Leer, 1969, 1980; Lomax, 1976; Patankar, 1980).

The importance of accurately representing a convective transport in a discrete space, which can be programmed in a digital computer, cannot be over emphasized, as several aspects of flow simulation depend directly on this (Drikakis and Rider, 2005; Drikakis, 2003; Hahn and Drikakis, 2005; Leschziner and Drikakis, 2002).

The errors involved in the discrete representation of a convective transport equation can assume different forms. Wave number analysis (Lomax et al., 2001) has been accepted as the most helpful way to not only understand the source of errors, but also to guide the design of new schemes based on target characteristics. It basically maps the convected variables and the discretized operators that prescribe their time evolution to the Fourier space, where, for each wave number, a complex amplification factor is found. This amplification factor corresponds to the transformation experienced by the convected quantity from one time step to the next, and should ideally match the analytic one, for all wave numbers, in both phase and amplitude. Errors in the phase are related to a spurious dispersive behavior, as generally different wave numbers will have different propagation speeds (convective speeds). Errors in the amplitude generally tend to damp the original wave forms and are associated with a diffusive behavior.

In the framework of Finite Difference Method (FDM)[1] in uniformly spaced mesh, it can be mathematically shown that unbiased centered schemes have zero diffusion. However, no matter how many points we choose to include in the stencil, there will always be some dispersive error. On the other hand, numerical schemes with some bias towards upwind, of which the famous first order *upwind* (Courant et al., 1952; Patankar, 1980) is a representative, invariably present spurious dissipation which damps the original wave form. It happens that with damping comes stabilization properties, and it is difficult to guarantee solution convergence without at least some level of dissipation, be it from upwind spurious effects or from some artificial viscosity explicitly added to the equations.

An endless debate among CFD practitioners is the one about how much *upwinding*, if any at all, must be used in a particular simulation. Throughout the history of CFD, the community has been trying to diminish the amount of *upwinding* to just the enough to guarantee meaningful solutions. Nowadays, the original "first order upwind" (UW1) is relegated to lesser roles, like that of quickly finding initial solutions, before switching to a more precise scheme and starting the definitive simulation.

As controversial as it might appear, we will show later on that the first order upwind is not the real responsible for the undesirable damping, and that it is actually possible to construct a scheme based on the same ideas – piecewise linear interpolation and approximation of first derivative by taking the difference between the point and its upwind neighbor – in a way that the resulting solution for the discrete system exactly matches the analytic one, with zero dissipation and zero dispersion.

The first and simplest problem where spurious effects can spoil the solution is the scalar convection. Let $\phi = \phi(t, x)$

---

[1]Throughout this paper, FDM was chosen to make the discussion clearer, although the ideas here presented may be transferred to other methods.

be a function representing the quantity to be convected, and for the sake of simplicity, let us consider the one dimension, linear, convective transport of ϕ, described by the following Partial Differential Equation (PDE):

$$\frac{\partial \phi}{\partial t} + u \frac{\partial \phi}{\partial x} = 0 \,, \tag{1}$$

where u is the flow velocity convecting ϕ. We shall initially assume u as a uniform and constant field in the following discussion.

In this case, the solution is simply $\phi(t,x) = \phi_0(x - ut)$, where $\phi_0(x) = \phi(0,x)$ is the initial wave form. Figure 1 illustrates an initial cosine wave and its convected version, 0.25 seconds later in a uniform velocity field with $u = 1m/s$.
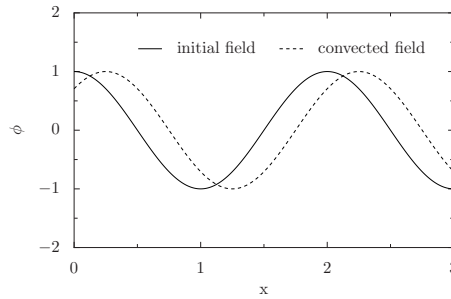

Figure 1. Convection of a cosine scalar field

The spatial derivative term in Eq. 1 can be discretized at the mesh sampling points x_j, in a traditional manner, as

$$\frac{\partial \phi}{\partial x}(x_j) \approx \frac{1}{\Delta x} \sum_{n=-N_s}^{N_s} a_n \phi(x_{j+n}) \,. \tag{2}$$

Here, the spatial derivative of ϕ is approximated at points x_j with a weighted sum of N_s neighbor values from each side, pondered by the corresponding coefficients, a_n. For the sake of simplicity, it is assumed that the sampling points are regularly distributed, $x_j = j\Delta x$, with Δx being the constant mesh spacing and j an integer number.

The spatially discretized version of Eq. 1 thus read:

$$\frac{\partial \phi}{\partial t} + u \frac{1}{\Delta x} \sum_{n=-N_s}^{N_s} a_n \phi(x_{j+n}) = 0 \,. \tag{3}$$

Defining the spatial Fourier transform of $\phi(t,x)$ as

$$\Phi(t,k) = \frac{1}{2\pi} \int_{-\infty}^{\infty} \phi(t,x) \exp\{-ikx\} dx \,, \tag{4}$$

and its inverse, as

$$\phi(t,x) = \int_{-\infty}^{\infty} \Phi(t,k) \exp\{ikx\} dk \,, \tag{5}$$

we can apply the transform to both sides of Eq. 1, yielding:

$$\frac{\partial \Phi}{\partial t} - iku\Phi = 0 \,, \tag{6}$$

where Φ is the Fourier transform of ϕ, $i = \sqrt{-1}$ is the pure imaginary number, and $k = 2\pi/\lambda$ is the wave number associated with the wavelength λ.

The spatially discretized version of Eq. 3, however, yields a different Fourier transform:

$$\frac{\partial \Phi}{\partial t} + u \frac{1}{\Delta x} \Phi \sum_{n=-N_s}^{N_s} a_n \exp\{ink\Delta x\} = 0 \,, \tag{7}$$

Comparing Eq. 6 and Eq. 7 it is clear that the discretized version has a different (or modified) wave number, $\bar{k}$, which can be written as:

$$\bar{k} = \frac{i}{\Delta x} \sum_{n=-N_s}^{N_s} a_n \exp\{ink\Delta x\} = 0 \,. \tag{8}$$

By adjusting or optimizing the coefficients a_n researchers have tailored the numerical schemes to their specific applications. However, some compromising is always needed in either performance or accuracy (Tam, 2004, 1995; Tam and Webb, 1993; Zhanxin et al., 2009; Hu et al., 1996; van Leer, 1986).

For instance, there are many situations in which the scalar ϕ is a physical quantity that cannot assume negative values, like when it represents temperature, specific mass, or turbulent kinetic energy. In those cases one might choose to sacrifice accuracy in capturing the right amount of damping (or lack of it) in order to guarantee that the solution is inside the physically acceptable limits (boundness property) Roe (1986, 1989); van Leer (1980). Very often, however, this compromise jeopardize the simulation, unless an extremely refined mesh is employed, which is not always possible.

That is exactly the case of several Reynolds Average Navier Stokes (RANS) models, where a transport equation for the kinetic energy is derived and its solution field is used to calculate the turbulent viscosity. If the kinetic energy becomes negative – as it probably will if unbounded schemes like central differences (CD) are used – the turbulent viscosity will also do so, and the solution will blow up. On the other hand too much dissipation damps the solution and can even become more significant than the physical modeling itself.

In turbulence numerical simulations the non-linearity in the Navier-Stokes equation is responsible for altering the wavelength of the structures, in accordance to the well-known direct energy cascade. Because not all wavelengths can be represented by the mesh, some of the structures are expected to gradually disappear, as their energy is transfered to unresolved modes. The problem with traditional numerical schemes is that they suffer a deterioration in performance as the mesh cut-off is approached, which affects the energy transfer rate even in smoother structures living in a resolved part of the spectrum. This weakness has triggered the development of physical subgrid models, as no numerical scheme until now could correctly represent the transfer of energy to unresolved modes without being too dissipative. In this paper we show that this limitation was actually related to the way the numerical schemes have been developed – in particular, to the error analysis tool used to understand and optimize them. Once we adopt a more physically driven approach, it becomes possible to develop numerical schemes that correctly predict the transfer of energy among modes without any spurious dissipation. If this is achieved, no physical modeling (or any other form of artificial dissipation) should be needed for the direct energy cascade, since the transfer of energy to unresolved structures would be exactly captured, meaning this part of the energy would naturally disappear.

In computational aeroacoustics (CAA) it is very important to accurately capture the amplitude and phase of the velocity and pressure fluctuations (Tam et al., 1993), as these will be the sources of sound. The delicate interference pattern and its sensitiveness to small errors (specially in phase) makes predicting the far field sound an extremely challenging task. A review of the main challenges, achievements and methods in aeroacoustics can be found in Tam (2004, 1995); Colonius and Lele (2004); Tam (2006); Kurbatskii and Mankbadi (2004).

An accurate numerical scheme is so important in this case that high order schemes using a fifteen points stencil in space and a 4th or 6th order Range-Kutta in time are often recommended (Allampalli et al., 2009; Zhanxin et al., 2009; Tam and Webb, 1993; Hu et al., 1996). These schemes are generally tailored to provide the desired characteristics, which is normally done by adjusting the coefficients a_n in Eq. 8 as well as the time discretization ones. An example of such scheme is the Dispertion Relation Preserving (DRP) (Tam and Webb, 1993; Bogey and Bailly, 2004). To avoid the appearance of spurious oscillations at the mesh cut-off frequency, a spatial filtering is often employed (Kurbatskii and Mankbadi, 2004) as an alternative to the use of an artificial selective damping (which can be provided either by an explicit term or by some embedded upwind bias, built in the algorithm).

It may at first seem impossible to develop a low order scheme that provides that level of accuracy required in CAA, but as we will show later on, a special first order upwind can be accurate to machine precision for uniform field, linear convective equations.

2. ERROR ANALYSIS

Wave number analysis is a very helpful tool in understanding the source of errors in discretization schemes and in designing improved versions. The analysis is done by taking an initial waveform at time t_0, decomposing it in Fourier modes, and, for each of these modes, examining the corresponding discretized solution at the next time step[2], $(t_0 + \Delta t)$. A combination of Lagrange and Fourier transform is normally used to analyze schemes when time is discretized (Tam, 1995, 2004), while Fourier transform alone is enough when time is treated continuously. An amplification factor in terms of amplitude and phase is given as the output, allowing us to understand the nature of the error for different wavelenghts, λ.

However, it is clear that this analysis is restricted to an interval $(t_0, t_0 + \Delta t)$ and does not take into account what happened before. Therefore, the predicted error is cumulative, and the numerical schemes developed based on it are deemed to be unable to capture features like the disappearance/reappearance of energy, as mentioned previously – once the solution is spoiled (damped, for instance), it will never recover the original form.

In this section we will explore other possibilities regarding the way the error of a certain numerical simulation is mea-

---

[2]If time is not discretized, but treated as a continuous differential, the analysis is still restricted to a local vicinity of t_0, sufficing to make $\Delta t \to 0$.

sured. The flowchart in Fig. 2 shows that there are several ways to obtain results for a convective transport, ranging from a purely analytical to a discrete solution. The convention used in this flowchart was the following: arrows with solid lines represent exact steps, such as solving a discretized system of equations (solving $Ax = b$ in matrix form), or finding the analytical solution of a Partial Differential Equation (PDE); arrows with dashed lines correspond to operations involving sampling at the mesh points followed or not by some kind of reconstruction (with a piecewise linear interpolation, for instance); arrows with dotted lines corresponds to some kind of modes decomposition, which in this paper will be the Fourier spectral decomposition. The six different results that can be obtained by the possible combinations of these operations are horizontally aligned, according to their compatibility. For instance, "Result 1" and "Result 2" can be compared to generate an error that will allow us to access how good one scheme is, based on the metric just defined. Results 3, 5 and 6 can also be compared, but Result 3 and Result 2 cannot, as they are incompatible.
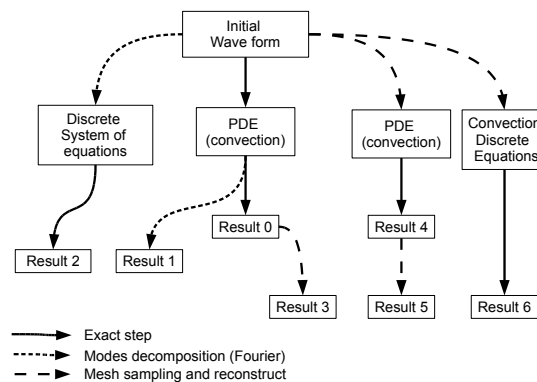

Figure 2. Different approaches for error analysis.

Referring to Fig. 2, the initial wave form can be applied to the PDE that exactly describes a convection phenomena. Solving this PDE yields "Result 0", which is the analytical solution, in the continuous form. The PDE could also be decomposed into Fourier modes and solved, generating the "Result 1", which gives the analytical expression for the amplification factor, for each wave number. "Result 1" is therefore the analytical solution in spectral space.

Each Fourier mode of an arbitrary initial wave form can be applied to the numerical discretization, resulting in a closed form expression ("Result 2") for an effective wave number, $\overline{k}$. In classical wave number analysis, this effective wave number provided by "Result 2" is compared to the exact one, obtained from the Fourier transform of the PDE ("Result 1").

"Result 3" is obtained after sampling the analytical solution ("Result 0") at the mesh points. This last operation will allow its comparison with other discrete results.

The initial wave form can also be immediately sampled at the mesh points and then reconstructed to a new continuous form. This reconstruction may involve piecewise linear interpolation for instance, or a more complex operation, like filtering. The new continuous form (reconstructed from the mesh-sampled data) can be fed to the original PDE representing the convective transport, which in turn has an analytical solution, labeled as "Result 4". To allow comparison to other discrete results, "Result 4" can be mesh-sampled and reconstructed if needed, yielding "Result 5".

The traditional discrete solution in physical space, "Result 6", is obtained by first sampling the initial wave form, and then applying it to the set of equations representing the convection transport in discretized form. Some reconstruction – like Taylor series – will be needed to approximate the spatial derivatives in these discretized equations. The exact solution of this discrete system is the numerical simulation result, labeled "Result 6".

One could then think about at least three different possibilities to study the error involved in the process of discretization:

1. Decompose the initial form into Fourier modes and apply the discretization to each of these modes, comparing the result to the Fourier modes of the final analytical solution. This is the classical wave number analysis and the correspondingly calculated error, which is the norm of the difference between "Result 2" and "Result 1", will be referred to as the "WN error".

2. The numerical simulation result ("Result 6") could be compared to a mesh-sampled version of the analytical solution ("Result 3"), instead of the pure analytical solution ("Result 0"). The corresponding error will be referred to as the "SAC error", standing for "Sampled Analytical Convection error", or the error when comparing against the Sampled analytical solution for the convection PDE.

3. Sample the initial quantity at the mesh points; reconstruct a continuous form and forget about the initial field; find an analytical solution ("Result 4") for the continuous convection equation, taking this reconstructed form as the initial condition; compare a sampled version ("Result 5") of "Result 4" to the discrete solution ("Result 6"). The error calculated this way will be referred to as the "RAC error", standing for "Reconstructed Analytically Convected", or the error when comparing against the analytical convection of a reconstructed initial field.

Each of these error definitions has its advantages and disadvantages. In the traditional wave number analysis, for instance, a closed expression for the "WN error" can be found for every spatial mode, which means that a single analysis (normally represented by a "$\overline{k} \times k$" graph) covers all possible initial wave forms. But as mentioned before, this analysis is restricted to a single time step, which means the error is cumulative over several of these intervals, and once the wave form is deformed, it will never recover its initial shape. This is usually the case, as it is not possible to achieve zero error at every wave number.

The "SAC" and "RAC" error analysis, on the other hand, has to be performed for a bunch of initial wave forms. This is because, at least for more general and complex numerical schemes, one cannot find a closed expression for the error as a function of the modal wave number. However, their advantage lies in the fact that the error is non-cumulative, as it is the measure of the difference between the analytical solution for the initially mesh-sampled wave form and the numerical solution, at any future times, independent of what happened at intermediate times. In this sense, zero error means that snapshots in future times (travelled distances being a multiple of Δx) will always match the analytical solution, no matter how far the convected distance was. Parameters like group velocity and amplitude will be exactly captured if the calculated error is zero.

Most optimizations of numerical schemes are performed by taking the error – generally the "WN error" – as the objective function to be minimized. Until now, the development of better numerical schemes were severely limited by this particular choice. An optimization based on "SAC" or "RAC" errors will lead to schemes more aligned with the convection physics.

To illustrate this, let us consider an arbitrary wave form, shown in Fig. 3, and its evolution according to a linear convective equation (Eq. 1), for uniform flow field, $u = 1m/s$. The snapshots correspond to the wave forms at $t = 0$, 0.5 and 1 seconds. The mesh acts as a sampling device that cannot read what is happening between two adjacent points, separated by $\Delta x = 1$ from each other. The initial wave form was purposely defined as an essentially pure *cosine* with some high frequency disturbance located between two mesh points, in such a way that it will be initially missed by the mesh.
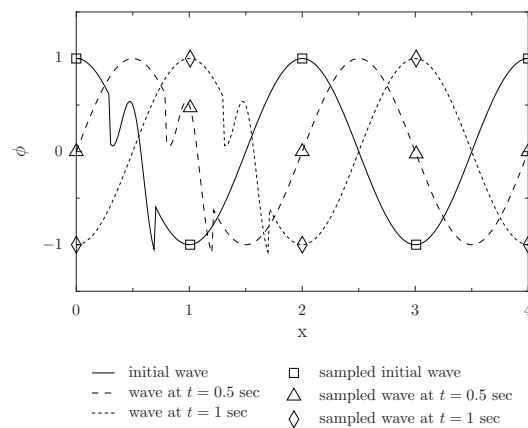

Figure 3. Convection of a scalar field and mesh-sampling.

In Fig. 3, the continuous, dashed, and dotted lines correspond to the analytical solutions – "Result 0" of the flowchart of Fig. 2 – at $t = 0$, $t = 0.5$ and $t = 1$, respectively. The symbols "□", "△", and "◇" represent the mesh-sampled wave form at the same instants of time, corresponding to "Result 3" of the flowchart.

In the particular case of the convection shown in Fig. 3, it is clear that mesh-sampling the final analytical solution – "Result 3" of the flowchart – yields a severely damped wave form at $t = 0.5$ seconds (△ symbol). This is the best this particular mesh could have done, even if a perfect numerical scheme was used. Clearly, if we choose to perform a rigorous wave number analysis, a lot of modes composing the complex oscillations in between nodes would have been missed even before the wave has travelled any distance. But if we take this approach (based on "Result 3") to define the error, we will be evaluating how far our discretized solution is from the result of the sampling applied to the analytical solution. Notice that, when the convected distance ($u\,t$) is a multiple of Δx, the original sampled wave form is recovered (◇ symbol), which shows that this error definition is not misleading at all.

This would not be the case if classical analysis was used instead: in Fig 3, the "WN error" for $t = 1$ would not be zero, even though the discretized solution exactly matches the sampled analytical solution. Actually, even for $t = 0$, before

any convection traveling is simulated, the traditional analysis already accuses the discrepancies due to the impossibility of capturing the high speed oscillations that happens between mesh nodes "0" and "1". One of the main contributions of this paper is to question this and to propose alternatives more aligned to the physical aspect of the transport. For this purpose, it must be now clear that one needs to distinguish the errors due to the reconstruction from the errors due to the transport simulation itself. Any optimization based on the error calculated by traditional wave number analysis will try to compensate for the missing modes, which in turn will spoil the solution at the mesh points. Therefore, if one tries to optimize the scheme by adjusting its coefficients relying entirely on classical analysis, chances are that the discretized solution becomes even farther apart from the sampled analytical solution ("Result 5").

Figure 4 illustrates the application of the continuous transport equation to a sampled and reconstructed version of the same initial field, corresponding to the set of operations leading to "Results 4" and, after a new sampling, "Result 5" in the flowchart. The continuous line represents the initial field, while the the square symbols with their connecting dotted lines represent its sampled and reconstructed version, when a piecewise linear interpolation is used. The "△" and "◇" symbols with their respective connecting lines corresponds to the "Result 5" of the flowchart at $t = 0.5$ and $t = 1$.
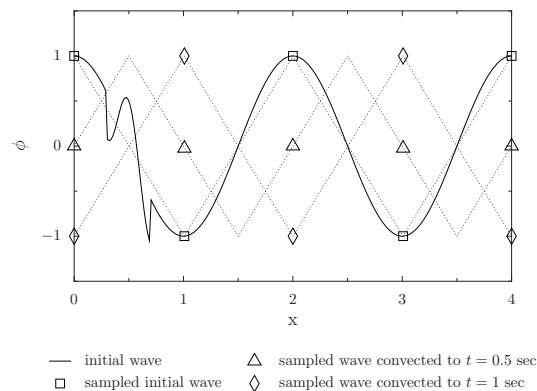

Figure 4. Convection of a reconstructed initial field.

Notice there is a subtle difference in the results of Fig. 3 and 4, for $t = 0.5$ at $x = 1$ ("△" symbol). This is due to the irreversible lost of information when the initial wave form is replaced by its sampled-reconstructed version. The original field disturbance observed from $x = 0.3$ to $x = 0.7$ (in between nodes 0 and 1) in Fig. 3 are completely lost after the piecewise linear reconstruction shown in Fig. 4, and can never be recovered again. At $t = 1$, however, both methods give exactly the same result. In fact, since the waves were initially coincident at the mesh nodes, the difference between "Result 3" and "Result 5" will be zero whenever the convected distance is a multiple of the mesh spacing Δx.

The rationale behind "SAC" and "RAC" error assessment is that one must accept that the mesh cannot exactly capture the complete Fourier modes of the analytical solution. By targeting the discretized versions of the analytical solution or the analytical solution of a discretized initial field, we are avoiding the inclusion of *aliasing* errors in our analysis, which is know to be a source of problems. In order words, separating the initial reconstruction error from the convection transport simulation errors allows one to accept the former and focus on the latter, which gives new perspectives in numerical simulation, as it will be shown later.

3. TOWARDS NON-DISSIPATIVE AND NON-DISPERSIVE SCHEMES

Once traditional wave number is substituted by a more physically driven one ("RAC" or "SAC"), some key observations about the simple linear convection of a wave form in a uniform field will set the foundations for the development of better schemes.

Referring again to Fig 1 or Fig. 4, it is clear that, as the wave is convected one time step (moves to the right), the spatial derivative at the mesh nodes must change from an initial value (equal to zero in this case) to some positive or negative value, depending on the location of the mesh node. That would be the expected result from analytical solution. On the other hand, if one takes a central differences discretization of this initial wave form, the term $\partial\phi/\partial x$ would be zero everywhere, which means, according to Eq. 1 (or Eq. 3), that no changes in ϕ will be noticed. While the literature recommends that *upwinding* should be completely avoided or kept to minimum levels, it is evident that some amount of bias in the discretization is needed to capture the physics of convection. It is not just a question of stability, which is indeed improved by *upwinding*, but more importantly, it seems that, without some form of *upwind* bias, an essential physical aspect of convection would be missed.

Observing the evolution of the wave form, in successive time steps, it is also clear that the spatial derivative to be used in the discretized equation should not be based on simple operations with node values. In Fig. 4, for instance, the spatial derivatives calculated at $t = 0.5$ would always be zero, no matter how large the computational stencil (N, in Eq. 2) is. The dotted line at this time clearly suggests that the derivative should be $\partial\phi/\partial x = 2$ for even nodes and $\partial\phi/\partial x = -2$ for

odd nodes.

Furthermore, taking the analytical convection of the piecewise linear reconstructed field (dotted lines in Fig. 4), one can notice that the spatial derivatives should be constant until the wave form has travelled one mesh space (Δx). Right after that, the derivative should change its value to become constant again, until the wave has travelled yet another mesh space – in this particular case shown in the same figure, the derivatives should change their sign. Of course, the fact that the derivative should be kept constant over periods of time and only seldom updated has to do with the piecewise linear reconstruction. Had a different reconstruction been chosen, like a high order polynomial, the derivative would have to be constantly changing, following the shape of the reconstructed wave.

All the points made above suggest that the spatial derivative should be an independent field, evolving according to its own transport equation. In the case of the Eq. 1, the spatial derivative transport equation is:

$$\frac{\partial G}{\partial t} + u\frac{\partial G}{\partial x} + \frac{\partial u}{\partial x}G = 0 \,;\text{with } G = \frac{\partial \phi}{\partial x}. \tag{9}$$

In the complete space of functions, Eq. 9 is redundant as it is derived from Eq. 1 – satisfying the latter automatically implies satisfying the former. However, in a truncated discrete environment, this is not the case, and Eq. 9 provides complementary information to the convective transport of ϕ. This (solving for an independent equation for the derivative) was the key missing link, absent in all previous numerical schemes of the literature.

To isolate the influences of the second and third terms in the left hand side of Eq. 9, we note that the third term becomes zero in a uniform flow field, while the second term becomes zero when ϕ is linear (G is constant).

The second term on the left hand side of Eq. 9 is the convection of G and accounts for the change in the spatial derivative (G) due to the shape of the reconstructed function, upon convection. This term alone has the ability to bring upwind information even if unbiased schemes are used in all spatial derivatives.

In a possible implementation of this new family of schemes based on a separate equation for the derivative G, a piecewise linear interpolation reconstructs the field between mesh nodes, taking as inputs the value of the primitive variable ϕ and of its derivative G. The evolution equation for G, when this particular reconstruction is used, will include an update step, for which first order upwind was used to evaluate G whenever required.

4. NUMERICAL EXPERIMENTS

In this section, preliminary results from two numerical experiments are presented in order to confirm the good properties expected from the new proposal.

In the first test, a simple linear convection in an uniform flow field is used to check if the new scheme has any spurious error. In the second test, a non-uniform field convection checks the new scheme capability of dealing with changes of wave lengths and the related transfer of energy towards unresolved modes.

4.1 Uniform field

For uniform convective velocity, the analytical solution for Eq. 1 is simply $\phi(t, x) = \phi(0, x - ut)$, meaning that the initial shape should be preserved as the wave travels by convection. Thus, for a convective distance multiple of the domain length, one expects the new field to be exactly coincident with the initial one, as the boundaries are linked as periodic.

Without lost of generality, the velocity is taken as $u = 1m/s$. The Courant number, $\eta = u\Delta t/\Delta x$ is the only parameter in the non-dimensional version of Eq. 1, and can be varied through changes in the time step, Δt.

A modulated Gaussian is taken as the initial field, and is obtained by multiplying a smooth bell-shaped waveform by $\cos(k_c x)$, with $k_c = 2\pi/\lambda_c$, yielding:

$$\phi = \cos(k_c x) \exp\left[-\log(2.0)\left[\frac{(x - x_0)}{r}\right]^2\right]. \tag{10}$$

The modulation operation (multiplication by the $\cos(k_c x)$) corresponds, in Fourier space, to a shift of the spectrum content, that will now be centered around k_c. A critical condition for all traditional schemes happens when λ_c gets close to $2\Delta x$. This initial wave resembles that of an amplitude modulated sound packet, whose carrier wave length is λ_c. One of the biggest challenges faced by modern Computational Aero Acoustics (CAA) is that a small mistake in either amplitude or phase of the numerical solution can significantly spoil the interference pattern at the far field and greatly alter the results.

For this test, the carrier wave number is set as the most critical one, $\lambda_c = 2\Delta x$. This means that the spectrum of the initial wave spans a wide range of frequencies, including the mesh cut-off mode, where all traditional discretization schemes are known to fail. The results when this initial wave is used are plotted in Fig. 5, and the corresponding normalized errors were of the order of machine precision (10^{-14}). The initial shape (centered at $x = 60$) and two evolution snapshots of the wave are displayed in the same figure. The dashed line corresponds to the snapshot at $t = 120$, exactly after the wave form has travelled one domain length, but it cannot be distinguished from the initial wave form. This attest

the excellent accuracy of the new proposal, as any dispersion or dissipative error would have deformed the wave during this long convection period.

This test used a time step $dt = 0.4$, resulting in a Courant number $\eta = 0.4$, which is a reasonably large Courant number for transient simulations.
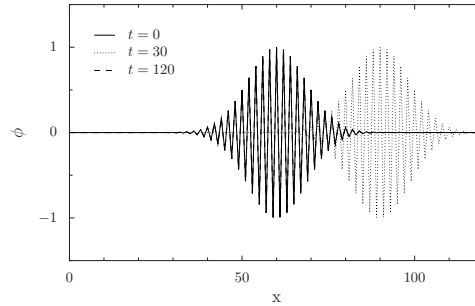

Figure 5. Test case 1h: ϕ at $t = 0$, 30 and 120 seconds

Exact solutions (1.46×10^{-16}) are also found for situations in which the Courant number is bigger (up to $\eta = 1$). The new proposal was not designed, however, for Courant numbers greater than one.

The performance of the new scheme up to now is encouraging, specially considering it is only first order in space and second order in time, at least according to traditional analysis. It must be now clear that classical error assessment tools have hampered the development of better numerical schemes, and new mathematical tools are needed. Most of the tests were run with low Courant number, in order to isolate the errors due to spatial discretization from those due to time discretization. Nonetheless, tests "1h" and "1i" pushed the limits to the extreme Courant allowed by the algorithm, and proved the new proposal is exact in all conditions involving a linear convection equation with uniform flow field. More stringent tests are however needed and are presented in the following sections.

4.2 Non-uniform field

The test cases proposed in this subsection aim at verifying the new scheme behavior when flow stretching/shrinking is present. The transport equation (Eq. 1), however, is still linear. The third term on the LHS of Eq. 9 is the responsible for capturing this phenomena, which could not be correctly reproduced by traditional schemes that only solves an equation for the primitive variable.

Therefore, in a non-uniform flow, the smallest eddies content of an initial waveform must naturally disappear if the numerical scheme is exact. Smoother structures, in turn, should be kept and suffer some distortions due to the convection in a non-uniform flow field.

In order to validate the new proposal in situations involving flow deformation, the flow field start with a region in which the flow presents a non-zero gradient, followed by a region of uniform flow, as described by the following equation

$$u(0, x) = \max[0.02x, 1] \ . \tag{11}$$

The initial field $\phi(0, x)$ was conceived to have a spread range of frequencies, including a high frequency carrier very close to the mesh limit, and a gaussian base form. A clipping operation zeros every negative value,

$$\phi(0, x) = \max\left[\cos(k_c x) \exp\left[-\log(2.0)\left[\frac{(x - x_0)}{r}\right]^2\right], 0\right] \ , \tag{12}$$

guaranteeing that the smooth content (obtained after some filtering operation) is non-zero.

Figure 6 displays the simulation results for four different schemes, including the new proposal, the 2nd order central differences (CD2), the Dispersion Relation Preserving with 7-points stencil with 4th order Runge-Kutta in time (DRP-7), and the DRP-15 (15 points stencil also with 4th order Runge-Kutta in time). The latter two schemes are specially designed for computational aeroacoustics and are far more complex then the new proposal. Snapshots of the wave evolution at $t = 42.86$ and 92.86, along with the initial wave ($t = 0$) are shown in the same figure. Additionally, the solution for the convection of an initially filtered version was also plotted ("$t = 92.86$ (filtered)"). This filtered version was obtained by taking the envelope of the wave and dividing by three, since two out of three sampled points are zeroed.

The traditional schemes (CD2, DRP-7 and DRP-15) presented a high content of spurious oscillations. The new proposal was immune to this problem, having captured the correct expansion of the smooth waveform, without any unphysical oscillation, as the high frequency modes naturally became unresolved and disappeared.

A subtle detail that can also be seen in Fig. 6(d) is worth of a comment: in the final wave form, the new proposal still presents some oscillations, mostly in the left part of the domain (from $x = 10$ to 60. These oscillations are not spurious
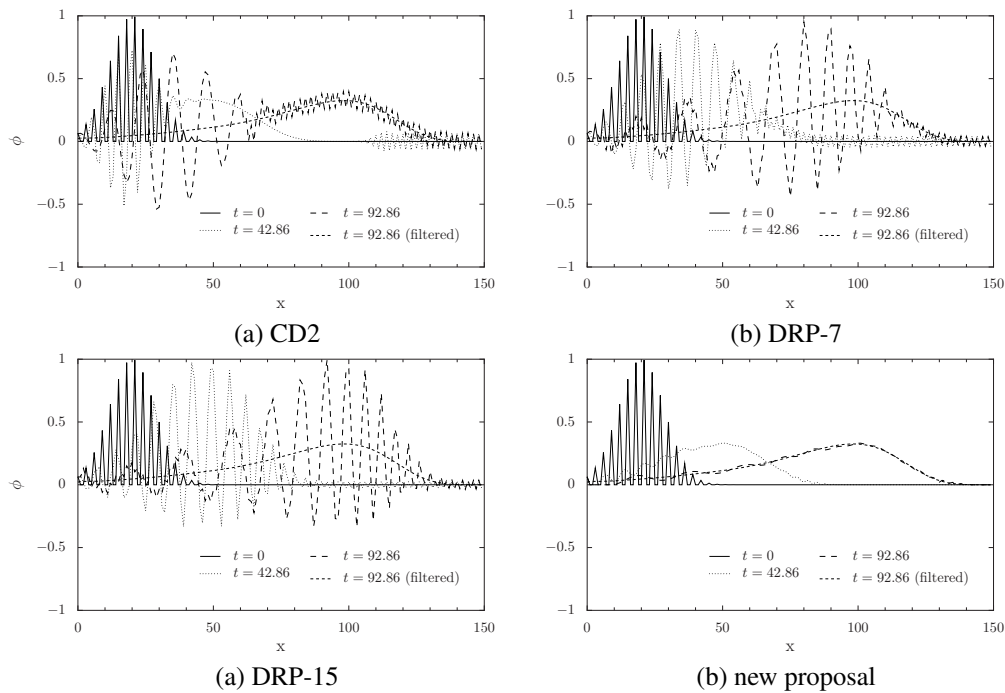
(a) CD2

(b) DRP-7

(a) DRP-15

(b) new proposal

Figure 6. Evolution of ϕ

or unphysical, as was the case with traditional schemes. They never made the value of ϕ become negative and are not as exaggerated as those of Fig. 6(a)-(c). Their origin seems to be related to a natural expansion of the initially short wavelengths, that luckily reached a value that could be represented by the mesh. This only confirms that the new proposal does not dissipate structures that still can be resolved by the mesh.

Fig. 7 shows the time evolution of the peak of ϕ as it travels through the flow gradient region and through the uniform field zone. While in the expansion zone, $0 < t < 42.86$, the high frequency content is damped and the peak of ϕ decreases. After this time, this peak stabilizes as there are no more changes in the wavelengths of the structures.
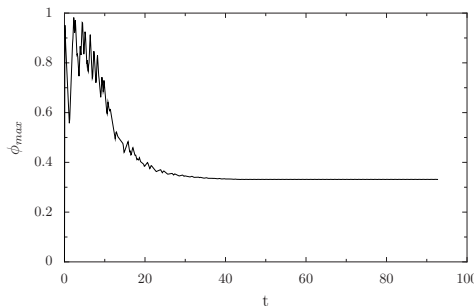

Figure 7. Evolution of ϕ_{max}

5. CONCLUSIONS

Traditional wave number analysis has been a helpful tool for the development and optimization of numerical schemes, but at the same time has some weakness points that have hampered the development of better discretization approaches.

Once a more physically driven error assessment tool was proposed, a new family of numerical schemes could be devised with special capabilities. In particular, it was shown that, in order to transfer energy towards unresolved modes, it was not necessary that the scheme was dissipative, as generally believed.

In fact, a new scheme built around first order upwind derivatives and piecewise linear reconstruction was shown to be not only non-dispersive and non-difusive, as it also presented the desired accuracy when transferring energy towards unresolved modes, without spoiling the resolved part of the spectrum. One can now realize that the first order upwind scheme was not the real responsible for the undesired dissipative characteristics he was known for. In the current proposal, in which an independent equation for the derivative of the primitive variable, the same first order approximation proved it was physically correct, as though when originally conceived to solve the earlier stabilization problems faced by rudimentary CFD codes.

Future extensions to full tridimensional Navier-Stokes may have a significant impact in key areas of computational physics, such as aeroacoustics and turbulence numerical simulation, where no more physical model should be needed for the direct cascade.

6. ACKNOWLEDGEMENTS

7. REFERENCES

Allampalli, V., Hixon, R., Nallasamy, M., and Sawyer, S. D. (2009). High-accuracy large-step explicit Runge-Kutta (HALE-RK) schemes for computational aeroacoustics. *Journal of Computational Physics*, 228(10):3837–3850.

Bogey, C. and Bailly, C. (2004). A family of low dispersive and low dissipative explicit schemes for flow and noise computations. *Journal of Computational Physics*, 194(1):194–214.

Colonius, T. and Lele, S. K. (2004). Computational aeroacoustics: progress on nonlinear problems of sound generation. *Progress in Aerospace Sciences*, 40:345–416.

Courant, R., Isaacson, E., and Rees, M. (1952). On the solution of nonlinear hyperbolic differential equations by finite differences. *Comm. Pure Appl. Math*, 5(3):243–255.

Drikakis, D. (2003). Advances in turbulent flow computations using high-resolution methods. *Progress in Aerospace Sciences*, 39(6-7):405–424.

Drikakis, D. and Rider, W. (2005). *High-resolution methods for incompressible and low-speed flows*. Springer.

Hahn, M. and Drikakis, D. (2005). Large eddy simulation of compressible turbulence using high-resolution methods. *International Journal for Numerical Methods in Fluids*, 47(8):971–977.

Hu, F. Q., Hussaini, M. Y., and Manthey, J. L. (1996). Low-dissipation and low-dispersion Runge-Kutta schemes for computational acoustics. *J. Comput. Phys.*, 124(1):177–191.

Kurbatskii, K. A. and Mankbadi, R. R. (2004). Review of computational aeroacoustics algorithms. *Int. J. Comput. Fluid Dyn.*, 18(6):533–546.

Leschziner, M. and Drikakis, D. (2002). Turbulence modelling and turbulent-flow computation in aeronautics. *Aeronautical Journal*, 106(1061):349–384.

Lomax, H. (1976). Recent progress in numerical techniques for flow simultation. *AIAA J.*, 14(4):512–518.

Lomax, H., Pulliam, T. H., and Zingg, D. W. (2001). *Fundamentals of computational fluid dynamics*. Scientific Computation. Springer-Verlag, Berlin.

Patankar, S. (1980). *Numerical heat transfer and fluid flow*. Hemisphere Pub.

Roe, P. L. (1986). A basis for upwind differencing of the two-dimensional unsteady Euler equations. In *Numerical methods for fluid dynamics, II*, volume 7 of *Inst. Math. Appl. Conf. Ser. New Ser.*, pages 55–80. Oxford Univ. Press, New York.

Roe, P. L. (1989). A survey of upwind differencing techniques. In *11th International Conference on Numerical Methods in Fluid Dynamics (Williamsburg, VA, 1988)*, volume 323 of *Lecture Notes in Phys.*, pages 69–78. Springer, Berlin.

Tam, C. (1995). Computational aeroacoustics: issues and methods. *AIAA Journal*, 33(10):1788–1796.

Tam, C. K. W. (2004). Computational aeroacoustics: an overview of computational challenges and applications. *Int. J. Comput. Fluid Dyn.*, 18(6):547–567.

Tam, C. K. W. (2006). Recent advances in computational aeroacoustics. *Fluid Dynam. Res.*, 38(9):591–615.

Tam, C. K. W. and Webb, J. C. (1993). Dispersion-relation-preserving finite difference schemes for computational acoustics. *J. Comput. Phys.*, 107(2):262–281.

Tam, C. K. W., Webb, J. C., and Dong, Z. (1993). A study of the short wave components in computational acoustics. *J. Comput. Acoust.*, 1(1):1–30.

van Leer, B. (1969). Stabilization of difference schemes for the equations of inviscid compressible flow by artificial diffusion. *J. Computational Phys.*, 3:473–485.

van Leer, B. (1980). Upwind differencing for hyperbolic systems of conservation laws. In *Numerical methods for engineering, 1 (Paris, 1980)*, pages 137–149. Dunod, Paris.

van Leer, B. (1986). On numerical dispersion by upwind differencing. *Appl. Numer. Math.*, 2(3-5):379–384.

Zhanxin, L., Qibai, H., Li, H., and Jixuan, Y. (2009). Optimized compact filtering schemes for computational aeroacoustics. *International Journal For Numerical Methods In Fluids*, 60(8):827–845.

8. Responsibility notice

The author is the only responsible for the printed material included in this paper